2023 62nd IEEE Conference on Decision and Control (CDC)
December 13-15, 2023. Marina Bay Sands, Singapore

Guidance for Terminal Direction and Final Time Constrained-Approach Towards a Moving Target

Vivek A[1] and Satadal Ghosh[1]

Abstract— **Approaching a moving target at a desired time along a desired orientation is an essential requirement for many applications. Most works that address this issue in the literature are developed considering a stationary target. Extending such guidance strategies against moving targets using the concept of predicted intercept point could degrade its performance. Instead, considering the engagement against a lower-speed moving but nonmaneuvering target directly, in this paper, a proportional navigation-based integrated guidance strategy is developed to address this problem of simultaneous control of terminal angle and final time. The desired terminal angle is achieved by suitably selecting the navigation gain and manipulating the lateral acceleration applied. At the same time, the final time requirement is satisfied by changing the purser's speed suitably. The proposed guidance scheme is validated through numerical simulations for different terminal requirements starting from same initial engagement geometry.**

I. Introduction

Traditionally, the objective of unmanned aerial vehicle (UAV) missions was centered on minimizing miss-distances or reaching predefined locations. However, the advancements in UAV technologies have increased UAV's usage and demand complex mission objectives. For example, applications such as formation flights, aerial deliveries, rendezvous, docking, and interdiction missions demand precise control over both terminal angle and time to achieve their objectives. Simultaneously controlling terminal angles and arrival times poses a difficult problem, which becomes even more challenging when the destination is not stationary. In this context, a guidance strategy for controlling the approach angle and time against a moving target is developed in this paper.

In the literature, simultaneous control of the terminal angle and final time have been formulated based on optimal control theory, known as optimal guidance laws (OGL) [1, 2], Sliding mode control (SMC) techniques [3–5]. Besides these, guidance strategies based on Proportional Navigation (PN) have been explored: Biased pure PN (PPN) with varying bias [6], and with navigation gain-switching [7, 8]. Trajectory shaping guidance laws presented in [9, 10] achieve the required objective by shaping a relevant variable as a polynomial function. Hybrid guidance strategies are also available in the literature: using OGL and time-to-go error feedback [11], using OGL and SMC [12], and using SMC and PN guidance [13].

Except for Ref. [4, 7, 10, 13], the fore-mentioned guidance laws are derived for engagements against stationary targets. Among them, [4, 7, 13] use the 'predicted intercept point' (PIP) concept, treating PIP as a virtual stationary target at each time step and using guidance laws initially designed for stationary targets. However, practically, estimating PIP is difficult due to uncertainties in target's states and time-to-go estimates. Reference [10], on the other hand, considered the look-angle dynamics as a polynomial function of time-to-go to achieve the dual objective. However, as a linear relation between downrange-to-go and time-to-go was used to derive the guidance strategy, this is effective mainly when the engagement geometry is closer to the collision triangle.

Note that OGLs mostly use linearized pursuer-target engagement geometry to derive the guidance commands and hence, are not suitable when the engagement is far away from the collision course. Besides, guidance strategies based on SMC often involve high-order derivatives and hard-to-measure variables, limiting their practicality. In contrast, the PN guidance is straightforward, relying solely on LOS rate measurements to generate the guidance commands. PN guidance is optimal and robust under certain conditions [14]. Hence, the PN-based guidance algorithm is considered in this paper. In addition, varying the pursuer's forward speed also could enhance its guidance performance. For example, drawing inspiration from the attacking strategy of the hawk which adapts its speed based on the prey's maneuver [15], the pursuer's speed has been varied for achieving interception with a maneuvering target in [16]. As UAVs of the present day have lesser sluggish control over their longitudinal acceleration compared to the bigger interceptors, varying forward speed plays a pivotal role in overall guidance strategies [16, 17].

This paper presents a novel multi-phase guidance strategy against lower-speed targets, integrating PN philosophy and speed variation to achieve both terminal direction and final time objectives considering nonlinear pursuer-target engagement. Unlike [7], which only adjusts navigation gain to satisfy the final time constraint, the longitudinal acceleration command is used here to achieve a broader range of final times. The two-phase PPN guidance (2pPPN) presented for constant speed pursuers in [18] is modified to handle varying pursuer speeds. The guidance strategy is validated through numerical simulations with approximated dynamics of a small UAV.

The remainder of this paper is organized as follows. Section II describes the problem setup and the objective. Section III gives the required background and explains how the longitudinal and lateral accelerations are generated to achieve the objectives. Numerical simulations in realistic conditions

[1]Vivek A and Satadal Ghosh are with the Department of Aerospace Engineering, Indian Institute of Technology Madras, Chennai-600036, India. ae19d005@smail.iitm.ac.in, satadal@iitm.ac.in

validate the developed guidance strategy in Section IV. Finally, the concluding remarks are given in Section V.

II. Problem Formulation and Preliminaries

A. Problem Description

Consider a planar engagement between a target T moving in a straight line (non-maneuvering) and a variable-speed pursuer P following PPN guidance as shown in Fig. 1. The pursuer and target are considered point masses. The pursuer is capable of generating longitudinal acceleration to vary its speed and lateral acceleration to change its heading direction. The target's speed and the heading angle are denoted by V_T and α_T, respectively. The pursuer's speed, heading angle, lateral acceleration, and longitudinal acceleration are denoted as V_P, α_P, a_P, and a_l, respectively. Also, lower-speed targets i.e., $\nu \triangleq V_P/V_T > 1$ is considered in this paper.

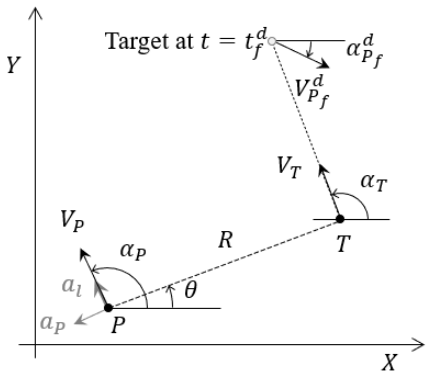

Fig. 1: Pursuer-target engagement geometry

The Line-of-Sight (LOS) range and angle between P and T are denoted as R and θ, respectively. Commanded, initial and final values are denoted with 'cmd', '0', and 'f'in subscript; desired value with 'd' in superscript. Considering ideal pursuer dynamics (no autopilot lag, i.e., $a_{P_{\rm cmd}} = a_P$ and $a_{l_{\rm cmd}} = a_l$), the kinematic equations governing the pursuer-target engagement are given as follows.

$$V_R = \dot{R} = V_T \cos(\alpha_T - \theta) - V_P \cos(\alpha_P - \theta), \quad (1)$$

$$V_\theta = R\dot{\theta} = V_T \sin(\alpha_T - \theta) - V_P \sin(\alpha_P - \theta), \quad (2)$$

$$\dot{\alpha}_P = a_P/V_P, \;\; \dot{V}_P = a_l \quad (3)$$

where, V_R and V_θ are the components of the relative velocity along and normal to the LOS, respectively. The PPN guidance law is considered for computing $a_{P_{\rm cmd}}$ given as

$$a_{P_{\rm cmd}} = N\, V_P\, \dot{\theta}. \quad (4)$$

Here, N is the navigation gain, which needs to be computed to generate a_P to control α_P and achieve the desired terminal angle $\alpha_{P_f}^d$. The $a_{l_{\rm cmd}}$ is considered as,

$$a_{l_{\rm cmd}} = \pm a_{l_{\max}} \quad (5)$$

where $a_{l_{\max}} > 0$ is the magnitude of the maximum longitudinal acceleration that the pursuer can generate. Here, $+a_{l_{\max}}$ refers to the acceleration applied along the direction of the pursuer's velocity vector, and $-a_{l_{\max}}$ refers to the opposite direction. To vary V_P, $\mathrm{sgn}(\mathrm{a}_{\mathrm{l}_{\mathrm{cmd}}})$ needs to be decided based on the difference between the desired final time t_f^d and the estimated final time $\hat{t}_f$.

The objective of this paper is to develop a PPN-based guidance strategy for a variable speed pursuer to approach a moving but non-maneuvering target along $\alpha_{P_f}^d$ at time t_f^d, by suitably adapting N and V_P.

B. Preliminaries of Terminal Angle Control

For constant-speed pursuers, the terminal angle achieved using PPN guidance can be expressed from (2) and (4) as,

$$\alpha_{P_f} = N\theta_f + (\alpha_{P_0} - N\theta_0), \quad (6)$$

From [19], the condition for bounded a_P against lower-speed targets at the end-game is given by $N \geq 2 + (2/\nu)$, where $\nu = V_P/V_T$. Thus, during the end-game, $N \in [2 + (2/\nu), \infty)$. Further, from (2), θ that forms the collision triangle for a given α_{P_f} is:

$$\theta_f = \tan^{-1}\left[\frac{\nu \sin\alpha_{P_f} - \sin\alpha_T}{\nu\cos\alpha_{P_f} - \cos\alpha_T}\right]. \quad (7)$$

Let $\alpha_{P_{f,1}}$ and $\alpha_{P_{f,2}}$ be the solutions obtained by solving Eqs. (6) and (7) for $N = 2 + (2/\nu)$, and ∞, respectively. Then, the following theorem gives the result on a two-phase PPN (2pPPN) guidance strategy to achieve any terminal angles in a half-plane against a moving but non-maneuvering target in 2-D engagement.

Theorem 1: For $\dot{\theta}_0 < 0$, a constant-speed pursuer following PPN guidance can attain any $\alpha_{P_f}^d \in \left[\alpha_{P_{f,1}}, \alpha_{P_{f,2}}\right)$ using $N = (\alpha_{P_f}^d - \alpha_{P_0})/(\theta_f^d - \theta_0) \geq 2 + (2/\nu)$, while $\alpha_{P_f}^d \in \left[\alpha_{P_{f,2}} - \pi, \alpha_{P_{f,1}}\right]$ can be achieved using a 2pPPN guidance as follows:

$$N = \begin{cases} N_{\rm ori} < \frac{\alpha_{P_f}^d - \alpha_{P_0}}{\theta_f^d - \theta_0}, & \text{if } \frac{\alpha_{P_f}^d - \alpha_P}{\theta_f^d - \theta} < 2 + \frac{2}{\nu} \\ \frac{\alpha_{P_f}^d - \alpha_P}{\theta_f^d - \theta}, & \text{if } \frac{\alpha_{P_f}^d - \alpha_P}{\theta_f^d - \theta} \geq 2 + \frac{2}{\nu} \end{cases} \quad (8)$$

where, θ_f^d is obtained from (7) as

$$\theta_f^d = \tan^{-1}\left[\frac{\nu \sin\alpha_{P_f}^d - \sin\alpha_T}{\nu\cos\alpha_{P_f}^d - \cos\alpha_T}\right]. \quad (9)$$

The proof of the above theorem follows a similar step as shown in [18], where the terminal angle control was considered for a special case of $\theta_0 = 0^\circ$ and $\alpha_T = 0^\circ$ against targets moving on surface. Hence, the proof of Theorem 1 is kept out of scope of this paper. When $\dot{\theta}_0 > 0$, the 2pPPN given in Theorem 1 can be used to achieve $\alpha_{P_f}^d \in \left(\alpha_{P_{f,2}}, \alpha_{P_{f,2}} + \pi\right]$. In this paper, this 2pPPN guidance given in Theorem 1 is adapted to consider a varying-speed pursuer. An additional phase is also added for final time control.

C. Preliminaries of Final Time Control

PN-based guidance strategies [7, 20–22] are available in the literature to control the final time by appropriately scheduling N based on $\hat{t}_f - t_f^d$. However, for applications where both t_f and α_{P_f} are constrained, varying only N to

satisfy both constraints restricts the spectrum of attainable t_f or α_{P_f}. Alternatively, V_P can also be varied to reach the desired collision configuration and achieve t_f^d, which was explored in [23] albeit without any terminal angle requirement. In the guidance formulation presented in this paper, both of N and V_P are to be varied suitably in an integrated way to satisfy the dual objective.

III. Guidance Strategy Development

This section details the final time control strategy and the guidance strategy for integrated terminal angle and final time control that form the main contribution of this paper.

A. Final Time Control

As mentioned in Section II-C, in this work, V_P is adapted to control t_f. The difference $\hat{t}_f - t_f^d$ is used for varying V_P. The required $\hat{t}_f$ information at any given time t is computed as follows.

$$\hat{t}_f = t + \hat{t}_{\text{go}}, \tag{10}$$

where, $\hat{t}_{\text{go}}$ is the estimate of time-to-go to reach T, computed at time t. If $(\alpha_{P_f}^d - \alpha_P(t))/(\theta_f^d - \theta(t)) \geq 2 + (2V_T/V_P(t))$, then $\hat{t}_{\text{go}}$ is computed directly using the numerical recursive time-to-go estimation algorithm as given by [24] using $N = (\alpha_{P_f}^d - \alpha_P(t))/(\theta_f^d - \theta(t))$. Otherwise, $\hat{t}_{\text{go}}$ is split into two components (both obtained by the numerical recursive time-to-go estimation algorithm [24]) as, $\hat{t}_{\text{go}} = \hat{t}_{\text{go}_1} + \hat{t}_{\text{go}_2}$, where $\hat{t}_{\text{go}_1}$ is the estimate of the time taken to complete the Orientation phase with $N = N_{\text{ori}}$ (see Eq. (8)), and $\hat{t}_{\text{go}_2}$ is the estimate of the time taken by P to reach T from the endpoint of the Orientation phase, with $N = 2 + (2V_T/V_P(t))$. Based on $\hat{t}_f$, the required $a_{l_{\text{cmd}}}$ to vary V_P is computed as,

$$a_{l_{\text{cmd}}} = \begin{cases} +a_{l_{\max}}, & \text{if } \hat{t}_f - t_f^d > \epsilon_t \\ 0\ , & \text{if } |\hat{t}_f - t_f^d| \leq \epsilon_t \\ -a_{l_{\max}}, & \text{if } \hat{t}_f - t_f^d < -\epsilon_t \end{cases} \tag{11}$$

where, ϵ_t is a pre-defined small threshold time. From (11), if $\hat{t}_f - t_f^d > \epsilon_t$, a positive $a_{l_{\text{cmd}}}$ is generated, which increases V_P, in turn, reduces the t_{go} to reach T satisfying the t_f^d criterion, and *vice versa*. Also, when $|\hat{t}_f - t_f^d| \leq \epsilon_t$, V_P is maintained constant.

Remark 1: Using $a_{l_{\text{cmd}}}$ as per (11) guarantees that $|\hat{t}_f - t_f^d| \leq \epsilon_t$ is achieved in a finite time.

By analyzing the variation of $\hat{t}_f$ for small initial heading error considering $t_{\text{go}}(t) = -R(t)/\dot{R}(t)$ and the linear variation in V_P due to $a_{l_{\text{cmd}}}$ as per (11), Remark 1 can be established. Numerical simulations also suggest that this remark also holds for larger initial heading errors. Further, using $a_{l_{\text{cmd}}}$ helps achieve the final time condition in a minimum time.

Remark 2: Varying V_P allows the pursuer to attain final times higher as well as lesser than $\hat{t}_f(0)$, where $\hat{t}_f(0)$ is the estimate of final time computed at $t = 0$. Thus, final times in the range $t_f^d \in [\hat{t}_f(0) - \Delta_1,\ \hat{t}_f(0) + \Delta_2]$ can be achieved using the proposed command. Here, Δ_1, and Δ_2 depend on the pursuer's kinematic constraints.

The proposed $a_{l_{\text{cmd}}}$ enables the pursuer to reach the target at time $t \in [t_f^d - \epsilon_t,\ t_f^d + \epsilon_t]$. It should be noted that the existing PN-based approach [7] based on varying N could only achieve a restrictive range of $t_f^d \geq \hat{t}_f(0)$, the guidance strategy proposed here helps to expand this range, and also facilitates achieving $t_f^d < \hat{t}_f(0)$ as noted in Remark 2.

B. Integrated Terminal Angle and Final Time Control

For pursuers with varying speeds, the 2pPPN guidance strategy discussed in Section II-B cannot be directly used, as the collision triangle condition (7) varies with the variation of V_P with time as governed by $a_{l_{cmd}}$ in (11). Hence, a PPN-based integrated guidance strategy consisting of three different phases (Orientation, Time-adjustment, and Final-PPN phases) to achieve the dual objective of achieving $\alpha_{P_f}^d$ and t_f^d is proposed in this section. Although the proposed strategy involves switching the guidance commands during the transition between phases, there is no continuum of discontinuities in the guidance commands over the time horizon. For better understanding, the flowchart of this guidance strategy is shown in Fig. 2.

1) Orientation phase: The purpose of the Orientation phase is to bring the pursuer to a $(\theta,\ \alpha_P)$ configuration such that $\alpha_{P_f}^d$ can be achieved with $N = (\alpha_{P_f}^d - \alpha_P)/(\theta_f^d - \theta) \geq 2 + (2/\nu)$, to ensure reaching T, with bounded a_P. However, as V_P needs to be varied for controlling t_f, ν also changes. Hence, for a given $\alpha_{P_f}^d$, from (9), the θ_f^d varies. Thus, the condition for exiting the Orientation phase is re-stated for varying V_P scenario as,

$$N_{\text{req}}(t) \triangleq \frac{\alpha_{P_f}^d - \alpha_P(t)}{\theta_f^d(t) - \theta(t)} \geq 2 + \frac{2\,V_T}{V_P(t)}. \tag{12}$$

We denote the condition given by (12) as the *terminal angle condition* to be satisfied in this paper. As shown in Fig. 2, initially, if the terminal angle condition is not satisfied, the pursuer enters the Orientation phase. During this phase, $a_{l_{\text{cmd}}}$ is generated as per (11), and $a_{P_{\text{cmd}}}$ is generated as per (4) with $N = N_{\text{ori}} < (\alpha_{P_f}^d - \alpha_P(t_{\text{ori}_0}))/(\theta_f^d(t_{\text{ori}_0}) - \theta(t_{\text{ori}_0}))$, where t_{ori_0} is the time, at which the Orientation phase is initiated. To guarantee that the terminal angle condition can be satisfied in finite time by following the proposed guidance commands for the varying V_P set-up under consideration in this paper, first, we show the evolution of θ_f^d and the required navigation gain, in the following results (Lemma 1, and 2).

Lemma 1: Applying $a_{l_{\text{cmd}}}$ as per (11) results in the change of θ_f^d as,

$$\text{sgn}(\dot{\theta}_f^d) = \begin{cases} \text{sgn}(\alpha_T - \alpha_{P_f}^d) & \text{if, } \hat{t}_f - t_f^d > \epsilon_t \\ -\text{sgn}(\alpha_T - \alpha_{P_f}^d) & \text{if, } \hat{t}_f - t_f^d < -\epsilon_t \end{cases} \tag{13}$$

By analyzing the variation of θ_f^d (given by (9)) with respect to V_P and variation of V_P with time, the sign of $\dot{\theta}_f^d$ given in Lemma 1 can be shown. Note that the variation of θ_f^d varies when V_P varies during the Orientation phase. Lemma 1 helps to analyze how N_{req} varies (refer to Lemma 2) and the condition given by (12) is affected due to variation in V_P.

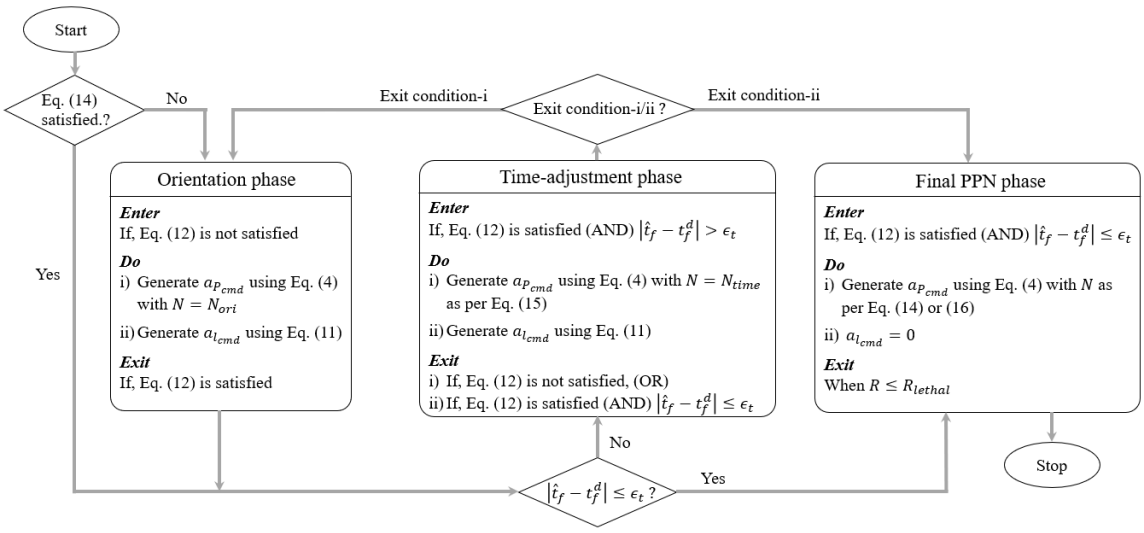

Fig. 2: Flowchart of the guidance algorithm

Lemma 2: During the Orientation phase, $\dot{N}_{\text{req}} > 0$, if $\text{sgn}(\dot{\theta})\,\text{sgn}(\dot{\theta}_f^d) = -1$.

Lemma 2 can be proved as follows. First, $\dot{N}_{\text{req}} > 0$ can be shown for a constant-speed pursuer by differentiating N_{req} (given in (12)) with respect to LOS angle θ and using $\text{sgn}(\dot{\theta})$. This result is then extended to Lemma 2 for a varying speed pursuer by using Lemma 1.

From Lemmas 1, 2, and Remark 1, the following result (Theorem 2) guarantees that the terminal angle condition can be achieved in finite time when V_P is varied using $a_{l_{\text{cmd}}}$ as per (11).

Theorem 2: A pursuer following the Orientation phase, with $a_{P_{\text{cmd}}}$ generated as per (4) with $N = N_{\text{ori}}$, and $a_{l_{\text{cmd}}}$ generated as per (11), will satisfy the terminal angle condition (12) in finite time.

Proof: Consider a case where $a_{l_{\text{cmd}}} = +a_{l_{\max}}$, i.e., V_P increases. From Lemma 2, if $\text{sgn}(\dot{\theta})\,\text{sgn}(\dot{\theta}_f^d) = -1$, then $\dot{N}_{\text{req}}(t) > 0$. Also, note that for increasing V_P as the right-hand side (RHS) of (12) monotonically decreases. Thus, from (12) and Lemma 2, it is clear that N_{req} increases and the terminal angle condition will be satisfied in a finite time.

For the other cases (i.e., $\text{sgn}(\dot{\theta})\,\text{sgn}(\dot{\theta}_f^d) = 1$, or decreasing V_P), recall from Remark 1 that the final time condition can be achieved in a finite time using the proposed $a_{l_{\text{cmd}}}$. So, once the final time condition is satisfied, V_P is maintained constant. As $\dot{N}_{\text{req}} > 0$ and the RHS of (12) is fixed for a constant-speed pursuer, the terminal angle condition will be satisfied in a finite time. ■

Thus, Theorem 2 guarantees that the terminal angle condition (12) is achieved, and the Orientation phase can be completed at some finite time $t = t_{\text{ori}_f}$. When the pursuer exits the Orientation phase, if $|\hat{t}_f - t_f^d| \leq \epsilon_t$, the Final PPN phase (refer to Fig. 2) is initiated with $N = N_{\text{final}}$ computed at $t = t_{\text{ori}_f}$ as

$$N_{\text{final}} = (\alpha_{P_f}^d - \alpha_P(t))/(\theta_f^d(t) - \theta(t))\Big|_{t=t_{\text{ori}_f}}. \quad (14)$$

Else, the Time-adjustment phase is initiated.

2) Time-adjustment phase: During this phase, V_P is continuously adjusted until $|\hat{t}_f - t_f^d| \leq \epsilon_t$. The $a_{l_{\text{cmd}}}$ is generated as per (11), and $a_{P_{\text{cmd}}}$ is generated as per (4) with the navigation gain $N = N_{\text{time}}(t)$ computed based on current states as,

$$N_{\text{time}}(t) = (\alpha_{P_f}^d - \alpha_P(t))/(\theta_f^d(t) - \theta(t)) \quad (15)$$

Recall that Remark 1 states that the final time condition can be achieved in a finite time. However, during the Time-adjustment phase, due to the variation of V_P with time, the terminal angle condition (12) may get violated. In that case, the pursuer re-enters the Orientation phase (refer to *Exit condition-i* in Fig. 2). Otherwise, the pursuer continues its Time-adjustment phase until the final time condition is satisfied at some time $t = t_{\text{tim}_f}$, and after that, enters the Final PPN phase (refer to *Exit condition-ii* in Fig. 2) with the final navigation gain computed at $t = t_{\text{tim}_f}$ as,

$$N_{\text{final}} = (\alpha_{P_f}^d - \alpha_P(t))/(\theta_f^d(t) - \theta(t))\Big|_{t=t_{\text{tim}_f}}. \quad (16)$$

If such a transition between the Orientation and Time-adjustment phases happens, the following proposition guarantees that such transitions end in finite time so that the Final PPN phase can be initiated then onward.

Proposition 1: The transfers between the Orientation phase and the time-adjustment phase end in finite time, and the engagement moves to the Final PPN phase when the final time condition is satisfied.

Proof: During the Time-adjustment phase, pursuer continuously applies a longitudinal acceleration $a_{l_{\text{cmd}}}$ generated as per (11), due to which V_P varies and in turn the RHS

of (12) varies. Due to this variation, the terminal angle condition could be violated, leading to a phase transition to the Orientation phase. However, from Remark 1, $|\hat{t}_f - t_f^d| \leq \epsilon_t$ is achieved in a finite time. Once this final time condition is satisfied, it will not be violated again as $\hat{t}_f$ is computed accurately considering all subsequent phases. Thus, the transitions from the Time-adjustment phase to the Orientation phase can only occur for a finite time interval until the final time condition is satisfied. When $|\hat{t}_f - t_f^d| \leq \epsilon_t$ is achieved during the Time-adjustment phase, the pursuer starts the Final-PPN phase with N_{final} as per (16). Else, if $|\hat{t}_f - t_f^d| \leq \epsilon_t$ is achieved during the Orientation phase, the pursuer enters the Final-PPN phase with N_{final} as per (14) immediately after completing its Orientation phase. Hence, the Proposition 1 is proved. ■

3) Final PPN phase: In the Final PPN phase, as shown in Fig. 2, $a_{l_{\text{cmd}}} = 0$. Only $a_{P_{\text{cmd}}}$ is generated as per (4) with the $N = N_{\text{final}}$ computed using (14) or (16) depending on its preceding phase. This ensures that $\alpha_{P_f}^d$ and t_f^d are achieved at the end of this phase. Theorem 3 below guarantees that the dual objectives stated in Section II-A are achieved by the presented multi-phase guidance scheme.

Theorem 3: A pursuer following the multi-phase PPN-based integrated guidance strategy with $a_{P_{\text{cmd}}}$ and $a_{l_{\text{cmd}}}$ as per Fig 2, is guaranteed to reach the target along $\alpha_{P_f}^d$ at time $t_f \in [t_f^d - \epsilon_t,\, t_f^d + \epsilon_t]$.

Proof: From Proposition 1, it is guaranteed that the transitions between the Time-adjustment and Orientation phases stop, and the Final PPN phase can be initiated in finite time. And, using fixed N in the Final PPN phase ((14) or (16)) allows the pursuer to attain $\alpha_{P_f} = \alpha_{P_f}^d$(Theorems 1, 2), and t_f sufficiently close to t_f^d (Remark 1) at the end of the Final PPN phase. ■

IV. Simulation Results

Numerical simulations are used to validate the terminal angle and final time-constrained guidance strategy presented in Section III. This validation is done under more realistic conditions to verify its real-time applicability. Typically, rotary-wing UAVs exhibit greater agility when compared to their fixed-wing counterparts. Thus, a small fixed-wing UAV which has an operating speed of $20 - 35\,\text{m/s}$, is considered for the numerical simulations [25]. The lags introduced by the autopilot, throttle/control surface dynamics and the flight dynamics are lumped together and considered as a first-order lag in realizing the generated $a_{l_{\text{cmd}}}$, and $a_{P_{\text{cmd}}}$ as follows.

$$\dot{a}_l = (a_{l_{\text{cmd}}} - a_l)/\tau_{a_l}; \quad \dot{a}_P = (a_{P_{\text{cmd}}} - a_P)/\tau_{a_P}. \quad (17)$$

Here, τ_{a_l} and τ_{a_P} are the lumped time constants corresponding to the forward speed loop and the coordinated turn loop, respectively. Typical values of these time constants for similar small fixed-wing UAVs are studied in the literature. In general, $\tau_{a_P} \in [0.01, 0.2]\,\text{s}$. And, the forward speed's dynamics is slower ($\tau_{a_l} \in [0.5, 1.5]\,\text{s}$) compared to the lateral dynamics [17, 26]. Hence, $\tau_{a_P} = 0.2\,\text{s}$, and $\tau_{a_l} = 1.5\,\text{s}$ are used for the simulation in this paper.

Simulations were performed in MATLAB R2022b with guidance command generated every $0.2\,\text{s}$. The following initial engagement conditions were used for the simulation: $(x_{P_0}, y_{P_0}) = (0,0)\,\text{m}$, $R_0 = 600\,\text{m}$, $\theta_0 = 0^\circ$, $V_{P_0} = 27\,\text{m/s}$, $\alpha_{P_0} = 75^\circ$, $V_T = 15\,\text{m/s}$, and $\alpha_T = 10^\circ$. Also, $N_{\text{ori}} = 1$, $a_{l_{\max}} = 1\,\text{m/s}^2$, $\epsilon_t = 2\,\text{s}$, and the mission is considered achieved when $R \leq R_{\text{lethal}} = 5\,\text{m}$. Also, $\alpha_{P_f}^d = \{-30^\circ, -90^\circ, -135^\circ\}$. These angles were within the capture region of the 2pPPN guidance strategy. The initial estimates of the final time corresponding to the aforementioned terminal angles were $\{82.3, 103.1, 107.0\}\,\text{s}$. So, the desired final times were chosen as $t_f^d = \{75, 120\}\,\text{s}$ to evaluate the performance of the guidance strategy against lower and higher t_f^d values.

The engagement trajectories are shown in Fig. 3a. From Fig. 3b, we note that as the terminal angle condition is not satisfied initially for all $\alpha_{P_f}^d$s, the engagement starts with the Orientation phase (i.e., $N = N_{\text{ori}}$) for all the cases. In addition, as $|\hat{t}_f - t_f^d| > \epsilon_t$ for all cases at the beginning of the engagement, to bring $\hat{t}_f$ closer to t_f^d, the pursuer's speed is adjusted by generating $a_{l_{\text{cmd}}}$ as per (11). The realized longitudinal acceleration and the corresponding change in V_P can be observed from Fig. 3c and 3e, respectively. At the end of the Orientation phase, as the final time criterion $|\,\hat{t}_f\big|_{t=t_{\text{ori}}} - t_f^d| < \epsilon_t$ is already satisfied for all the cases, the engagement enters the Final PPN phase (instead of the Time-adjustment phase) for all cases. Also, Fig. 3d shows that a_P is bounded even when the lags are considered. Further, from Fig. 3f (transition between phases), it can be observed that there are no Time-adjustment phases for the given scenarios. From the actually achieved terminal configurations listed in Table I, we notice that $|t_f - t_f^d| < \epsilon_t$ and $\alpha_{P_f} \approx \alpha_{P_f}^d$.

TABLE I: Achieved final times and terminal angles

α_{P_f}, deg	$t_f^d = 75\,\text{s}$		$t_f^d = 120\,\text{s}$	
	α_{P_f}, deg	t_f, s	α_{P_f}, deg	t_f, s
-30	-29.8	75.9	-29.8	118.8
-90	-89.7	75.6	-89.8	119.2
-135	-135.3	74.4	-135.4	118.7

Futher, from Fig. 3c, a few isolated pulses can be observed during the Orientation phase. This is because of the following reason: the final time condition is continuously verified throughout the Orientation phase even when $\left|\hat{t}_f(t) - t_f^d\right| \leq \epsilon_t$. So, any small error in computing $\hat{t}_f$ could impact the final time condition which was already achieved, and the $a_{l_{\text{cmd}}}$ is generated whenever $\left|\hat{t}_f(t) - t_f^d\right| > \epsilon_t$. Furthermore, no chattering is observed in the outputs, despite the acceleration commands generated by this multi-phase guidance strategy being discontinuous at the transition of phases. This indicates that the proposed multi-phase strategy is applicable in practical scenarios.

V. Conclusion

This paper develops a PPN-based multi-phase integrated guidance strategy to approach a moving but nonmaneuvering

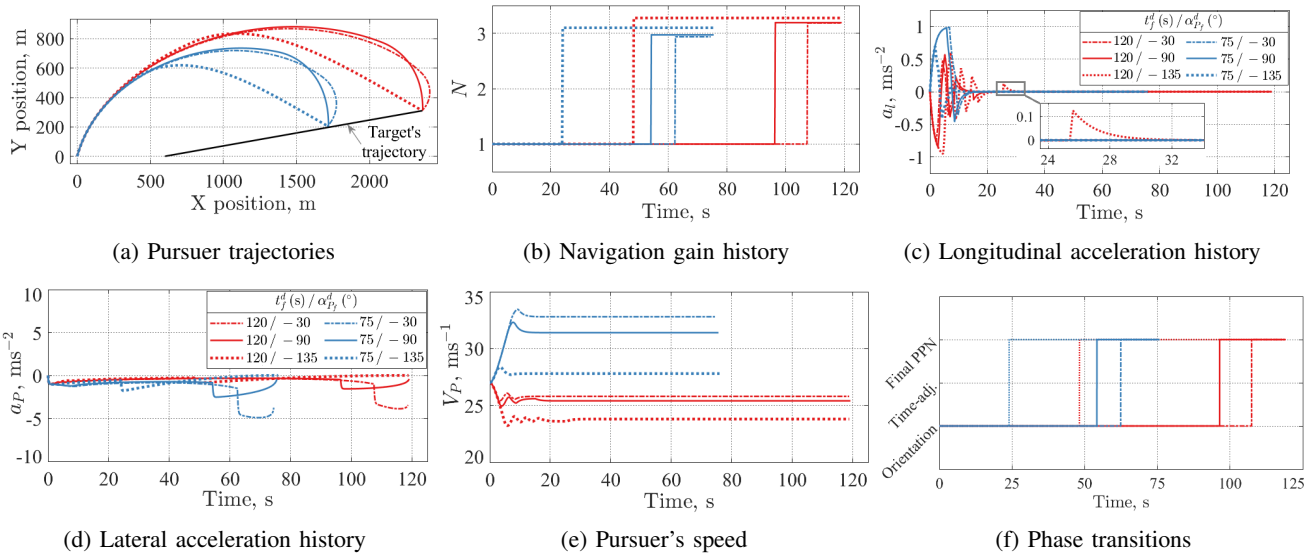

(a) Pursuer trajectories (b) Navigation gain history (c) Longitudinal acceleration history

(d) Lateral acceleration history (e) Pursuer's speed (f) Phase transitions

Fig. 3: Simulation results - with $t_f^d = \{75, 120\}$ s, and $\alpha_{P_f}^d = \{-30°, -90°, -135°\}$.

target along a desired orientation at a desired final time. Given an initial pursuer orientation, the desired terminal orientation lie in a specific half-space of angles, while the desired final time could be both more and less than the initial time-to-go estimates. Qualitative analysis has been provided for achievable terminal angles and final times ranges under a time-varying pursuer's speed set-up. Simulation results under realistic conditions have been found to validate the theoretical findings of the developed guidance scheme. Extending the range of achievable terminal angles and adapting this guidance scheme for a salvo attack mission form the future scope of this research.

REFERENCES

[1] J.-I. Lee, I.-S. Jeon, and M.-J. Tahk, "Guidance law to control impact time and angle," *IEEE Trans. Aerosp. Electron. Syst.*, vol. 43, pp. 301–310, Jan. 2007.

[2] K. S. Erer and R. Tekin, "Impact time and angle control based on constrained optimal solutions," *J. Guid. Control Dyn.*, vol. 39, pp. 2448–2454, Oct. 2016.

[3] J. Song, S. Song, and S. Xu, "Three-dimensional cooperative guidance law for multiple missiles with finite-time convergence," *Aerosp. Sci. Technol.*, vol. 67, pp. 193–205, Aug. 2017.

[4] S. R. Kumar and D. Ghose, "Sliding mode guidance for impact time and angle constraints," *Proc. Inst. Mech. Eng. G: J. Aerosp. Eng.*, vol. 232, no. 16, pp. 2961–2977, 2018.

[5] X. Chen and J. Wang, "Sliding-mode guidance for simultaneous control of impact time and angle," *J. Guid. Control Dyn.*, vol. 42, pp. 394–401, Feb. 2019.

[6] Y. Zhang, G. Ma, and A. Liu, "Guidance law with impact time and impact angle constraints," *Chin. J. Aeronaut.*, vol. 26, pp. 960–966, Aug. 2013.

[7] H. A. See, S. Ghosh, and O. Yakimenko, "Towards the development of an autonomous interdiction capability for unmanned aerial systems," in *Proc. 2017 Int. Conf. Unmanned Aircr. Syst.*, IEEE, June 2017.

[8] A. Vivek and S. Ghosh, "A guidance for simultaneous formation about a stationary point," in *AIAA SCITECH 2023 Forum*, AIAA, Jan. 2023.

[9] Y. Zhao, Y. Sheng, and X. Liu, "Trajectory reshaping based guidance with impact time and angle constraints," *Chin. J. Aeronaut.*, vol. 29, no. 4, pp. 984–994, 2016.

[10] R. Tekin and K. S. Erer, "Impact time and angle control against moving targets with look angle shaping," *J. Guid. Control Dyn.*, vol. 43, pp. 1020–1025, May 2020.

[11] S.-W. Shim, S.-M. Hong, G.-H. Moon, and M.-J. Tahk, "Impact angle and time control guidance under field-of-view constraints and maneuver limits," *Int. J. Aeronaut. Space Sci.*, vol. 19, pp. 217–226, Mar. 2018.

[12] X. Chen and J. Wang, "Optimal control based guidance law to control both impact time and impact angle," *Aerosp. Sci. Technol.*, vol. 84, pp. 454–463, Jan. 2019.

[13] Q. Hu, T. Han, and M. Xin, "New impact time and angle guidance strategy via virtual target approach," *J. Guid. Control Dyn.*, vol. 41, pp. 1755–1765, Aug. 2018.

[14] P. Zarchan, *Tactical and Strategic Missile Guidance, Sixth Edition*. AIAA, Mar. 2012.

[15] C. H. Brighton and G. K. Taylor, "Hawks steer attacks using a guidance system tuned for close pursuit of erratically manoeuvring targets," *Nat. Commun.*, vol. 10, June 2019.

[16] N. Paul and D. Ghose, "Longitudinal-acceleration-based guidance law for maneuvering targets inspired by hawk's attack strategy," *J. Guid. Control Dyn.*, pp. 1–11, Feb. 2023.

[17] G. Ducard and H. P. Geering, "Airspeed control for unmanned aerial vehicles: a nonlinear dynamic inversion approach," in *2008 16th Mediterranean Conference on Control and Automation*, IEEE, June 2008.

[18] A. Ratnoo and D. Ghose, "Impact angle constrained guidance against nonstationary nonmaneuvering targets," *J. Guid. Control Dyn.*, vol. 33, pp. 269–275, Jan. 2010.

[19] M. Guelman, "A qualitative study of proportional navigation," *IEEE Trans. Aerosp. Electron. Syst.*, vol. AES-7, pp. 637–643, July 1971.

[20] I.-S. Jeon, J.-I. Lee, and M.-J. Tahk, "Homing guidance law for cooperative attack of multiple missiles," *J. Guid. Control Dyn.*, vol. 33, pp. 275–280, Jan. 2010.

[21] S. Ghosh, D. Ghose, and S. Raha, "Three dimensional retro-PN based impact time control for higher speed nonmaneuvering targets," in *Proc. IEEE 52nd Conf. Decis. Control. (CDC)*, IEEE, Dec. 2013.

[22] S. Ghosh, D. Ghose, and S. Raha, "Retro-PN based simultaneous salvo attack against higher speed nonmaneuvering targets," *IFAC Proceedings Volumes*, vol. 47, no. 1, pp. 34–40, 2014.

[23] Y.-S. Jung, J.-I. Lee, C.-H. Lee, and M.-J. Tahk, "A new collision control guidance law based on speed control for kill vehicles," *Int. J. Aeronaut. Space Sci.*, vol. 20, pp. 792–805, Feb. 2019.

[24] S. Ghosh, D. Ghose, and S. Raha, "Unified time-to-go algorithms for proportional navigation class of guidance," *J. Guid. Control Dyn.*, vol. 39, no. 6, pp. 1188–1205, 2016.

[25] TextronSystems, "Aerosonde Fixed Wing - Specifications." https://www.textronsystems.com/products/aerosonde, Accessed on Mar 05, 2023.

[26] A. M. Kamal, A. Bayoumy, and A. Elshabka, "Modeling and flight simulation of unmanned aerial vehicle enhanced with fine tuning," *Aerosp. Sci. Technol.*, vol. 51, pp. 106–117, Apr. 2016.